

Research Article

A Class of Fourth-Order Telegraph-Diffusion Equations for Image Restoration

Weili Zeng,¹ Xiaobo Lu,² and Xianghua Tan³

¹ ITS Research Center, School of Transportation, Southeast University, Nanjing 210096, China

² School of Automation, Southeast University, Nanjing 210096, China

³ School of Mathematics and Computer Science, Hunan Normal University, Nanjing 210096, China

Correspondence should be addressed to Xiaobo Lu, xblu2008@yahoo.cn

Received 14 March 2011; Revised 17 May 2011; Accepted 2 June 2011

Academic Editor: E. S. Van Vleck

Copyright © 2011 Weili Zeng et al. This is an open access article distributed under the Creative Commons Attribution License, which permits unrestricted use, distribution, and reproduction in any medium, provided the original work is properly cited.

A class of nonlinear fourth-order telegraph-diffusion equations (TDE) for image restoration are proposed based on fourth-order TDE and bilateral filtering. The proposed model enjoys the benefits of both fourth-order TDE and bilateral filtering, which is not only edge preserving and robust to noise but also avoids the staircase effects. The existence, uniqueness, and stability of the solution for our model are proved. Experiment results show the effectiveness of the proposed model and demonstrate its superiority to the existing models.

1. Introduction

The use of second-order partial differential equations (PDE) has been studied as a useful tool for image restoration (noise removal). They include anisotropic diffusion equations [1–3] and total variation models [4] as well as curve evolution equations [5]. These second-order techniques have been proved to be effective for removing noise without causing excessive smoothing of the edges. However, the images resulting from these techniques are often piecewise constant, and therefore, the processed image will look “blocky” [6–8]. To reduce the blocky effect, while preserving sharp jump discontinuities, many methods in the literature [9–21] have been proposed to solve the problem.

A rather detailed analysis of blocky effects associated with anisotropic diffusion which was carried out in [6]. Let u denote the image intensity function, t the time, the anisotropic diffusion equation as formulated by Perona and Malik [1] presented as (the PM model)

$$u_t - \nabla \cdot (g(|\nabla u|)\nabla u) = 0, \quad (1.1)$$

where g is the conductance coefficient, $\nabla \cdot$ and ∇ denote the divergence and the gradient, respectively. Equation (1.1) is associated with the following energy functional:

$$E(u) = \int_{\Omega} f(|\nabla u|) d\Omega, \quad (1.2)$$

where Ω is the image support, and $f(\cdot) \geq 0$ is an increasing function associated with the diffusion coefficient as

$$g(s) = \frac{f'(\sqrt{s})}{\sqrt{s}}. \quad (1.3)$$

The PM model is then associated with an energy-dissipating process that seeks the minimum of the energy functional. From energy functional (1.2), it is obvious that level images are the global minima of the energy functional. Detailed analysis in [6] indicates that when there is no backward diffusion, a level image is the only minimum of the energy functional, so PM model will evolve toward the formation of a level image function. Since PM model is designed such that smooth areas are diffused faster than less smooth ones, blocky effects will appear in the early stage of diffusion even though all the blocks will finally merge to form a level image. Similarly, when there is backward diffusion, however, any piecewise level image is a global minimum of the energy functional, so blocks will appear in the early stage of the diffusion and will.

In 2000, You and Kaveh [12] proposed the following fourth-order PDE (the YK model)

$$u_t + \nabla^2 \left(g \left(\left| \nabla^2 u \right| \right) \nabla^2 u \right) = 0, \quad (1.4)$$

where ∇^2 denotes Laplace operator. The YK model replaces the gradient operator in PM model with a Laplace operator. Due to the fact that the Laplace of an image at a pixel is zero only if the image is planar in its neighborhood, the YK fourth-order PDE attempts to remove noise and preserve edges by approximating an observed image with a piecewise planar image. It is well known that piecewise smooth images look more natural than the piecewise constant images. Therefore, the blocky effect will be reduced and the image will look more nature. However, fourth-order PDE has an inherent limitation. The proposed PDE tends to leave images with speckle artifacts.

Recently, Ratner and Zeevi [22] introduced the following *telegraph-diffusion* equation (TDE model)

$$u_{tt} + \lambda u_t - \nabla \cdot (g(|\nabla u|) \nabla u) = 0, \quad (1.5)$$

where λ is the damping coefficient and g is the elasticity coefficient. Note that the TDE model is derived from (1.1) by adding second time derivative of the image. It is interesting to note that (1.5) converges to the diffusion equation (1.1) not only for large λ and g , but also after very long time [5, 6]. While one may find when the noise is large, (1.5) will be unstable in presence of noise which is similar to that of the PM model [1]. In order to overcome this

drawback, most recently, Cao et al. [23] proposed the following *improved telegraph-diffusion* equation (ITDE model)

$$u_{tt} + \lambda u_t - \nabla \cdot (g_1(|\nabla G_\sigma * u|)\nabla u) = 0, \quad (1.6)$$

where G_σ is a Gaussian filtering. The TDE model (1.5), together with its improved version (1.6), has certain drawbacks. Since the model uses anisotropic diffusion, the filter inherits the staircase effects of anisotropic diffusion. The Gaussian filtering is not a perfect filtering method. Moreover, since the model uses anisotropic diffusion, the filter inherits the block effects of anisotropic diffusion.

Inspired by the ideas of [12, 22], it is natural to investigate a model inherits the advantages of the YK model and TDE model. Our proposed fourth-order telegraph-diffusion equation as follows:

$$u_{tt} + \lambda u_t + \nabla^2 \left(g_2 \left(\left| \nabla^2 u \right| \right) \nabla^2 u \right) = 0, \quad (1.7)$$

where ∇^2 denotes Laplace operator. To our best knowledge, second-order derivative is sensitive to the noise. While one may find when the image is very noisy, (1.7) will be unstable which could not distinguish correctly the “true” edges and “false” edges. Considering that we can eliminate some noise before solving model (1.6), we reformulate model (1.6) as follows:

$$u_{tt} + \lambda u_t + \nabla^2 \left(g_3 \left(\left| \nabla^2 B_\sigma(u) \right| \right) \nabla^2 u \right) = 0, \quad (1.8)$$

where B_σ is a bilateral filtering [24, 25]; namely,

$$B_\sigma(u(x)) = \frac{1}{W(x)} \int_{\Omega} G_{\sigma_s}(\xi, x) G_{\sigma_r}(u(\xi), u(x)) u(\xi) d\xi, \quad (1.9)$$

with the normalization constant

$$W(x) = \int_{\Omega} G_{\sigma_s}(\xi, x) G_{\sigma_r}(u(\xi), u(x)) d\xi, \quad (1.10)$$

where G_{σ_s} will be a spatial Gaussian that decreases the influence of distant pixels, while G_{σ_r} will be a range Gaussian that decreases the influence of pixels ξ with intensity values that are very different from those of $u(x)$; for example,

$$G_{\sigma_s} = \exp\left(-\frac{|\xi - x|^2}{2\sigma_s^2}\right), \quad G_{\sigma_r} = \exp\left(-\frac{|u(\xi) - u(x)|^2}{2\sigma_r^2}\right), \quad (1.11)$$

where parameters σ_s and σ_r dictate the amount of filtering applied in the domain and the range of the image, respectively.

The ability of edge preservation in the fourth-order TDE-based image restoration method strongly depends on the conductance coefficient g . The desirable conductance

coefficient should be diffused more in smooth areas and less around less intensity transitions, so that small variations in image intensity such as noise and unwanted texture are smoothed and edges are preserved. In the implementation of our proposed method, we use the following function:

$$g_3(s) = \frac{1}{\sqrt{1 + (s/k)^2}}, \quad (1.12)$$

where k is a threshold constant.

We will recall that the main purpose of the function g is to provide adaptive smoothing. It should not only precisely locate the position of the main edges, but it should also inhibit diffusion at edges. This is exactly what bilateral filtering accomplishes. It is proposed as a tool to reduce noise and preserve edges, by means of exploiting all relevant neighborhoods. It combines gray levels not only based on their gray similarity but also their geometric closeness and prefers near values to distant values in both domain and range.

The remainder of this paper is organized as follows. In Section 2, we will show the existence and uniqueness of our proposed model. Section 3 presents a discredited numerical implementation of the proposed model. Numerical experiments are presented in Section 4, and the paper is concluded in Section 5.

2. Analysis of Our Proposed Model: Existence and Uniqueness of Weak Solutions

In this section, we establish the existence and uniqueness of the following problem:

$$u_{tt} + \lambda u_t + \nabla^2 \left(g \left(\left| \nabla^2 B_\sigma(u) \right| \right) \nabla^2 u \right) = 0, \quad (x, t) \in \Omega_T = \Omega \times (0, T), \quad (2.1)$$

$$u(x, 0) = u_0(x), \quad u_t(x, 0) = 0, \quad x \in \Omega, \quad (2.2)$$

$$u = 0, \quad \frac{\partial u}{\partial n} = 0, \quad (x, t) \in \partial\Omega \times (0, T), \quad (2.3)$$

where Ω is a bounded domain of \mathbb{R}^N with an appropriately smooth boundary, n denotes the unit outer normal to Ω , and $T > 0$. In this section, C will represent a generic constant that may change from line to line even if in the same inequality.

The following standard notations are used throughout. We denote $H^k(\Omega)$ is a Hilbert space for the norm

$$\|u\|_{H^k(\Omega)} := \left(\sum_{|s| \leq k} \int_{\Omega} \left| \frac{\partial^m u}{\partial x^m} \right|^2 dx \right)^{1/2}, \quad (2.4)$$

where k is a positive integer and $\partial^m u / \partial x^m$ of order $|m| = \sum_{j=1}^m m_j \leq k$ denotes the distributional derivative of u .

We denote by $L^p(0, T; H^k(\Omega))$ the set of all functions u such that for almost every t in $(0, T)$, $u(t)$ belongs to $H^k(\Omega)$. $L^p(0, T; H^k(\Omega))$ is a normed space for the norm

$$\|u\|_{L^p(0, T, H^k(\Omega))} := \begin{cases} \left(\int_0^T \|u(t)\|_{H^k(\Omega)}^p dt \right)^{1/p}, & (1 \leq p < \infty), \\ \text{ess sup}_{0 \leq t \leq T} \|u(t)\|_{H^k(\Omega)}, & (p = \infty), \end{cases} \quad (2.5)$$

where k is a positive integer. $L^\infty(0, T; L^2(\Omega))$ is a normed space for the norm

$$\|u\|_{L^\infty(0, T, L^2(\Omega))} := \text{ess sup}_{0 \leq t \leq T} \|u(t)\|_{L^2(\Omega)}. \quad (2.6)$$

We denote by $H^2(\Omega)'$ the dual of $H^2(\Omega)$ and introduce the following function space $V(\Omega)$

$$V(\Omega) = \left\{ u \in H^2(\Omega) : u = 0, \frac{\partial u}{\partial n}, x \in \partial\Omega \right\}. \quad (2.7)$$

Obviously, $V(\Omega)$ is a Banach space with the norm $\|\cdot\|_{V(\Omega)} = \|\cdot\|_{H^2(\Omega)}$.

Definition 2.1. Let T be a fixed positive number. A function u is a weak solution of the problem (2.1)–(2.3) provided

- (i) $u \in C([0, T]; L^2(\Omega)) \cap L^\infty(0, T; V)$, $u_t \in L^\infty(0, T; L^2(\Omega))$ and $u_{tt} \in L^\infty(0, T; V')$,
- (ii) $\int_\Omega u_{tt}\varphi + \lambda \int_\Omega u_t\varphi + \int_\Omega g(|\Delta B_\sigma * w|)\Delta u\Delta\varphi = 0$
for any $\varphi \in V(\Omega)$ and a. e. time $0 \leq t \leq T$,
- (iii) $u(0) = u_0$, $u_t(0) = 0$.

2.1. Fourth-Order Linear Equation: Existence and Uniqueness

Now, we consider the existence and uniqueness of weak solutions of the following linear TD problem

$$u_{tt} + \lambda u_t + \nabla^2 \left(g \left(\left| \nabla^2 B_\sigma(w) \right| \right) \nabla^2 u \right) = 0, \quad (x, t) \in \Omega_T = \Omega \times (0, T), \quad (2.8)$$

$$u(x, 0) = u_0(x), \quad u_t(x, 0) = 0, \quad x \in \Omega, \quad (2.9)$$

$$u = 0, \quad \frac{\partial u}{\partial n} = 0, \quad (x, t) \in \partial\Omega \times (0, T), \quad (2.10)$$

where $w \in L^\infty([0, T]; L^2(\Omega))$.

Definition 2.2. A function u_w is called a weak solution of the problem (2.8)–(2.10) provided

- (i) $u_w \in C([0, T]; L^2(\Omega)) \cap L^\infty(0, T; V)$, $(u_w)_t \in L^\infty(0, T; L^2(\Omega))$ and $(u_w)_{tt} \in L^2(0, T; V')$,
- (ii) $\int_\Omega (u_w)_{tt}\varphi dx + \lambda \int_\Omega (u_w)_t\varphi dx + \int_\Omega g(|\nabla^2 B_\sigma * w|)\nabla^2 u_w \nabla^2 \varphi dx = 0$
for any $\varphi \in V(\Omega)$ and a. e. $0 \leq t \leq T$,
- (iii) $u(0) = u_0$, $u_t(0) = 0$.

Theorem 2.3. Suppose that $w \in L^\infty([0, T]; L^2(\Omega))$ and $u_0 \in H^2(\Omega)$, then the problem (2.8)–(2.10) admits a unique weak solution u_w .

In order to prove Theorem 2.3, we will prove the following two lemmas.

Lemma 2.4. Suppose that $u \in L^2(\Omega)$, then there exists a constant $C_1 > 0$, depending only on σ , $|\Omega|$ and N , such that

$$\left\| \nabla^2 B_\sigma(u) \right\|_{L^\infty(\Omega)} \leq C_1 \|u\|_{L^2(\Omega)}. \quad (2.11)$$

Moreover, there exists a constant $C_2 > 0$, depending only on σ , $|\Omega|$, n such that

$$\left\| g\left(\left|\nabla^2 B_\sigma(u)\right|\right) - g\left(\left|\nabla^2 B_\sigma(v)\right|\right) \right\|_{L^\infty(\Omega)} \leq C_2 \|u - v\|_{L^2(\Omega)}, \quad (2.12)$$

for each $u, v \in L^2(\Omega)$.

Proof. By the definition of B_σ in (1.8), we then calculate

$$\begin{aligned} \left\| \nabla^2 B_\sigma(u) \right\|_{L^\infty(\Omega)} &= \frac{1}{W(x)} \int_\Omega \left| \exp\left(-\frac{|\xi - x|}{2\sigma_s^2}\right) \right| \left| \exp\left(-\frac{|u(\xi) - u(x)|}{2\sigma_r^2}\right) \right| |u(\xi)| d\xi \\ &\leq C(|\Omega|, \sigma, N) \|u\|_{L^2(\Omega)} \int_\Omega \left| \exp\left(-\frac{|\xi - x|}{2\sigma_s^2}\right) \right| \left| \exp\left(-\frac{|u(\xi) - u(x)|}{2\sigma_r^2}\right) \right| d\xi \\ &\leq C_1 \|u\|_{L^2(\Omega)}. \end{aligned} \quad (2.13)$$

Moreover, since $g(s)$ and B_σ are smooth, we have

$$\begin{aligned} \left\| g\left(\left|\nabla^2 B_\sigma(u)\right|\right) - g\left(\left|\nabla^2 B_\sigma(v)\right|\right) \right\|_{L^\infty(\Omega)} &\leq C \left\| \left|\nabla^2 B_\sigma(u)\right|^2 - \left|\nabla^2 B_\sigma(v)\right|^2 \right\|_{L^\infty(\Omega)} \\ &\leq C \left\| \left|\nabla^2 B_\sigma(u)\right| + \left|\nabla^2 B_\sigma(v)\right| \right\|_{L^\infty(\Omega)} \left\| \nabla^2 B_\sigma(u - v) \right\|_{L^\infty(\Omega)} \\ &= C(|\Omega|, \sigma, N) \left(\|u\|_{L^2(\Omega)} + \|v\|_{L^2(\Omega)} \right) \|u - v\|_{L^2(\Omega)} \\ &\leq C_2 \|u - v\|_{L^2(\Omega)}. \end{aligned} \quad (2.14)$$

Therefore, we draw the conclusion. \square

Lemma 2.5. If there exists $M > 0$ such that

$$\|\mathbf{w}\|_{L^\infty(0, T; L^2(\Omega))} + \|\mathbf{w}_t\|_{L^\infty(0, T; L^2(\Omega))} \leq M. \quad (2.15)$$

Then, one has the estimate

$$\|u(t)\|_{L^\infty(0,T;H^2(\Omega))} + \|u_t(t)\|_{L^\infty(0,T;L^2(\Omega))} + \|u_{tt}\|_{L^2(0,T;V')} \leq C\|u_0\|_{H^2(\Omega)}. \quad (2.16)$$

Proof. Multiplying (2.8) by u_t and integrating over Ω yields

$$\frac{1}{2} \frac{d}{dt} \int_{\Omega} (u_t)^2 dx + \lambda \int_{\Omega} (u_t)^2 dx + \int_{\Omega} g\left(|\nabla^2 B_\sigma(w)|\right) \nabla^2 u \nabla^2 u_t dx = 0, \quad (2.17)$$

for a.e. $0 \leq t \leq T$.

Note that

$$\begin{aligned} \int_{\Omega} g\left(|\nabla^2 B_\sigma(w)|\right) \Delta u \Delta u_t dx &= \frac{d}{dt} \left(\frac{1}{2} \int_{\Omega} g\left(|\nabla^2 B_\sigma(w)|\right) (\nabla^2 u)^2 dx \right) \\ &\quad - \frac{1}{2} \int_{\Omega} g_t\left(|\nabla^2 B_\sigma(w)|\right) (\nabla^2 u)^2 dx. \end{aligned} \quad (2.18)$$

Since w and w_t satisfy (2.15), then $\nabla^2 B_\sigma(w)$, $\nabla^2 B_\sigma(w_t)$ belong to $L^\infty(0, T; L^\infty(\Omega))$ and there exists a constant C depending on B_σ and Ω such that

$$\begin{aligned} \left\| \nabla^2 B_\sigma(w) \right\|_{L^\infty(0,T;L^\infty(\Omega))} &\leq C\|u_0\|_{H^2(\Omega)}, \\ \left\| \nabla^2 B_\sigma(w_t) \right\|_{L^\infty(0,T;L^\infty(\Omega))} &\leq C\|u_0\|_{H^2(\Omega)}, \end{aligned} \quad (2.19)$$

for any $x \in V$, a.e. $0 \leq t \leq T$. Therefore, since g is decreasing and $t \rightarrow g(\sqrt{t})$ is smooth, there exist two constants $\alpha, \beta > 0$ such that

$$\alpha \leq g\left(|\nabla^2 B_\sigma(w)|\right) \leq 1, \quad \left| g_t\left(|\nabla^2 B_\sigma(w)|\right) \right| \leq \beta\|u_0\|_{H^2(\Omega)}, \quad (2.20)$$

for any $x \in \Omega$, a.e. $0 \leq t \leq T$.

Consequently, (2.18) yields

$$\int_{\Omega} g\left(|\nabla^2 B_\sigma * w|\right) \Delta u \Delta u_t dx \geq \frac{\alpha}{2} \frac{d}{dt} \left(\int_{\Omega} (\nabla^2 u)^2 dx \right) - C\|u\|_{H^2(\Omega)}^2. \quad (2.21)$$

In terms of (2.17) and (2.21), it then follows that

$$\frac{d}{dt} \left(\|u_t\|_{L^2(\Omega)}^2 + \|u\|_{H^2(\Omega)}^2 \right) \leq C \left(\|u_t\|_{L^2(\Omega)}^2 + \|u\|_{H^2(\Omega)}^2 \right), \quad (2.22)$$

for a.e. $0 \leq t \leq T$.

Now, write

$$\eta(t) = \|u_t\|_{L^2(\Omega)}^2 + \|u\|_{H^2(\Omega)}^2. \quad (2.23)$$

Then, (2.22) reads

$$\eta'(t) \leq C\eta(t), \quad (2.24)$$

for a.e. $0 \leq t \leq T$. Applying the Gronwall inequality to (2.24) yields the estimate

$$\eta(t) \leq e^{Ct}\eta(0), \quad 0 \leq t \leq T. \quad (2.25)$$

Since

$$\eta(0) = \|u_t(0)\|_{L^2(\Omega)}^2 + \|u(0)\|_{H^2(\Omega)}^2 = \|u(0)\|_{H^2(\Omega)}^2, \quad (2.26)$$

we obtain from (2.23)–(2.25) the estimate

$$\|u(t)\|_{L^\infty(0,T;H^2(\Omega))} + \|u_t(t)\|_{L^\infty(0,T;L^2(\Omega))} \leq C\|u_0\|_{H^2(\Omega)}^2. \quad (2.27)$$

Multiplying (2.8) by φ and integrating over Ω , we deduce for a.e. $0 \leq t \leq T$ that

$$\int_{\Omega} u_{tt}\varphi \, dx + \lambda \int_{\Omega} u_t\varphi \, dx + \int_{\Omega} g\left(\left|\nabla^2 B_\sigma * w\right|\right) \nabla^2 u \nabla^2 \varphi \, dx = 0, \quad (2.28)$$

where $\varphi \in H_0^2(\Omega)$ and $\|\varphi\|_{H_0^2(\Omega)} \leq 1$.

Consequently,

$$\|u_{tt}\|_{V'} \leq C\|u\|_{H^2(\Omega)}. \quad (2.29)$$

Therefore,

$$\int_0^T \|u_{tt}\|_{V'}^2 \, dt \leq C \int_0^T \|u\|_{H^2(\Omega)}^2 \, dt \leq C\|u_0\|_{H^2(\Omega)}^2. \quad (2.30)$$

This completes the proof of the lemma. \square

Remark 2.6. By Lemma 2.5, Theorem 2.3 can be proved by the Galerkin method (see [22]). Here, we omit the details of the proof of Theorem 2.3.

2.2. Fourth-Order Nonlinear Equation: Existence and Uniqueness

Theorem 2.7 (see ([26], Schauder's Fixed Point Theorem)). *Suppose that X denotes a real Banach space and $K \subset X$ is compact and convex, and assume also that*

$$S : K \longrightarrow X \quad (2.31)$$

is continuous. Then, S has a fixed point in K .

Theorem 2.8. *Suppose that $u_0 \in H^2(\Omega)$, then the problem (2.1)–(2.3) admits one and only one weak solution.*

Proof. In the following, we prove the theorem in two parts.

(1) *Existence of a Solution*

In this first section, we show the existence of a weak solution of (2.1)–(2.3) by Schauder's fixed point theorem [22] and Theorem 2.3. We introduce the space

$$W(0, T) = \left\{ w \in L^\infty(0, T; H^2(\Omega)), w_t \in L^\infty(0, T; L^2(\Omega)), w_{tt} \in L^\infty(0, T; H^2(\Omega)') \right\}. \quad (2.32)$$

Obviously, $W(0, T)$ is a Banach space with the norm

$$\|w\|_{W(0, T)} = \|w\|_{L^\infty(0, T; H^2(\Omega))} + \|w_t\|_{L^\infty(0, T; L^2(\Omega))} + \|w_{tt}\|_{L^\infty(0, T; H^2(\Omega)')}. \quad (2.33)$$

Recalling Lemma 2.5, we introduce the subspace W_0 of $W(0, T)$ defined by

$$W_0 = \left\{ w \in W(0, T); w(0) = u_0, w_t(0) = 0, \|w\|_{L^\infty(0, T; L^2(\Omega))} + \|w_t\|_{L^\infty(0, T; L^2(\Omega))} + \|w_{tt}\|_{L^2(0, T; V')} \leq C \|u_0\|_{H^2(\Omega)} \right\}. \quad (2.34)$$

By construction, $S : w \rightarrow u_w$ is a mapping from W_0 into W_0 . Since $W(0, T)$ is compactly imbedded in $L^2(0, T; L^2(\Omega))$, W_0 is a nonempty, convex, and weakly compact subset of $L^2(0, T; L^2(\Omega))$.

In order to apply the Schauder fixed point theorem, we need to prove that S is a continuous compact mapping from W_0 into W_0 . Let $\{w_k\}$ be a sequence in W_0 which converges weakly to some w in W_0 and $u_k = S(w_k)$. We have to prove that $S(w_k) = u_k$ converges weakly to $S(w) = u_w$. By using the classical theorem of compact inclusion in Sobolev spaces [27], the sequence $\{w_k\}$ contains a subsequence (still denoted by) $\{w_k\}$ and $\{u_k\}$ contains a subsequence (still denoted by) $\{u_k\}$ such that

$$w_k \rightarrow w \quad \text{in } L^2(0, T; L^2(\Omega)) \text{ and a.e. on } \Omega \times (0, T), \quad (2.35)$$

$$g(|\nabla^2 B_\sigma * w_k|) \rightarrow g(|\nabla^2 B_\sigma * w|) \quad \text{in } L^2(0, T; L^2(\Omega)) \text{ and a.e. on } \Omega_T, \quad (2.36)$$

$$u_k \rightarrow u \quad \text{in } L^2(0, T; H^2(\Omega)), \quad (2.37)$$

$$(u_k)_t \rightarrow (u)_t \quad \text{weakly in } L^2(0, T; L^2(\Omega)), \quad (2.38)$$

$$(u_k)_{tt} \rightharpoonup (u)_{tt} \text{ weakly in } L^2(0, T; V'), \quad (2.39)$$

$$\nabla^2 u_k \rightharpoonup \nabla^2 u \text{ weakly in } L^2(0, T; L^2(\Omega)), \quad (2.40)$$

$$u_k(x, 0) \rightarrow u(x, 0) \text{ in } L^2(\Omega), \quad (2.41)$$

$$(u_k)_t(x, 0) \rightarrow 0 \text{ in } V'. \quad (2.42)$$

Since $\{u_k\}$ is the weak solutions of (2.8)–(2.10) corresponding to $\{w_k\}$, we have, for a.e. $0 \leq t \leq T$

$$\int_{\Omega} (u_k)_{tt} \varphi dx + \lambda \int_{\Omega} (u_k)_t \varphi dx + \int_{\Omega} g(|\nabla^2 B_{\sigma}(w_k)|) \nabla^2 u_k \nabla^2 \varphi dx = 0. \quad (2.43)$$

Integrating (2.43) from 0 to T yields

$$\int_0^T \int_{\Omega} (u_k)_{tt} \varphi dx dt + \lambda \int_0^T \int_{\Omega} (u_k)_t \varphi dx dt + \int_0^T \int_{\Omega} g(|\nabla^2 B_{\sigma}(w_k)|) \nabla^2 u_k \nabla^2 \varphi dx dt = 0. \quad (2.44)$$

From (2.38)–(2.39), we have

$$\int_0^T \int_{\Omega} (u_k)_{tt} \varphi dx dt \rightarrow \int_0^T \int_{\Omega} (u)_{tt} \varphi dx dt, \text{ as } k \rightarrow \infty, \quad (2.45)$$

$$\lambda \int_0^T \int_{\Omega} (u_k)_t \varphi dx dt \rightarrow \lambda \int_0^T \int_{\Omega} (u)_t \varphi dx dt. \quad (2.46)$$

Considering the third term in (2.44)

$$\begin{aligned} & \left| \int_0^T \int_{\Omega} g(|\nabla^2 B_{\sigma}(w_k)|) \nabla^2 u_k \nabla^2 \varphi dx dt - \int_0^T \int_{\Omega} g(|\nabla^2 B_{\sigma}(w)|) \Delta u \Delta \varphi dx dt \right| \\ & \leq \int_0^T \int_{\Omega} |g(|\nabla^2 B_{\sigma}(w_k)|) - g(|\nabla^2 B_{\sigma}(w)|)| \Delta u_k \Delta \varphi dx dt \\ & \quad + \left| \int_0^T \int_{\Omega} g(|\nabla^2 B_{\sigma}(w_k)|) \nabla^2 (u_k - u) \nabla^2 \varphi dx dt \right| = A + B. \end{aligned} \quad (2.47)$$

According to Lemma 2.4 and (2.40), we deduce, as $k \rightarrow \infty$

$$A \leq C \int_0^T \int_{\Omega} \|w_k - w\|_{L^2(\Omega)} |\Delta u_k| |\Delta \varphi| \leq C(\varphi) \|w_k - w\|_{L^2(\Omega)} \|\Delta u_k\|_{L^2(0, T; L^2(\Omega))} \rightarrow 0, \quad (2.48)$$

and note also, as $k \rightarrow \infty$, $B \rightarrow \infty$.

Letting $k \rightarrow \infty$ in (2.44) yields

$$\int_0^T \int_{\Omega} (u)_{tt} \varphi \, dx \, dt + \lambda \int_0^T \int_{\Omega} (u)_t \varphi \, dx \, dt + \int_0^T \int_{\Omega} g\left(|\nabla^2 B_{\sigma}(w)|\right) \nabla^2 u \nabla^2 \varphi \, dx \, dt = 0. \quad (2.49)$$

Therefore, by the arbitrariness of $\varphi \in V$, we obtain, for a.e. $t \in [0, T]$

$$\int_{\Omega} (u)_{tt} \varphi \, dx + \lambda \int_{\Omega} (u)_t \varphi \, dx + \int_{\Omega} g\left(|\nabla^2 B_{\sigma}(w)|\right) \nabla^2 u \nabla^2 \varphi \, dx = 0, \quad (2.50)$$

which implies

$$u = u_w = S(w). \quad (2.51)$$

By the uniqueness of the solution of linear problem (2.8)–(2.10) and (2.37), the sequence $u_k = S(w_k)$ converges weakly in W_0 to $u = S(w)$. Hence, the mapping S is weakly continuous from W_0 into W_0 . This in turn shows that mapping S is compact. A similar argument shows that S is a continuous mapping. Applying the Schauder fixed point theorem, we conclude that S has a fixed point $u = S(u)$, which consequently solve (2.1)–(2.3). Using the classical theory of parabolic equations and the bootstrap argument [26], we can deduce that u is a strong solution of (1.1)–(1.4) and $u \in C^{\infty}((0, T) \times \Omega)$.

(2) Uniqueness of the Solution

Now, we turn to the proof of the uniqueness, following the idea in [22]. Let u_1 and u_2 be two solutions of (2.1)–(2.3), and we have, for almost every t in $[0, T]$ and $i = 1, 2$

$$(u_1 - u_2)_{tt} + \lambda(u_1 - u_2)_t + \nabla^2(\beta_1 \nabla^2(u_1 - u_2)) = \nabla^2((\beta_1 - \beta_2) \nabla^2 u_2), \quad (x, t) \in \Omega_T, \quad (2.52)$$

$$u_i(x, 0) = u_0(x), \quad \frac{\partial u_i}{\partial t}(x, 0) = 0, \quad x \in \Omega, \quad (2.53)$$

$$u_i = 0, \quad \frac{\partial u_i}{\partial n} = 0, \quad (x, t) \in \partial\Omega \times (0, T), \quad (2.54)$$

in the distribution sense, where

$$\beta_i(t) = g\left(|\nabla^2 B_{\sigma} * u_i|\right). \quad (2.55)$$

It suffices to show that $u_1 - u_2 \equiv 0$. To verify this, fix $0 < s < T$ and set

$$v_i(t) = \begin{cases} \int_t^s u_i(\tau) d\tau, & 0 < t \leq s, \\ 0, & s \leq t < T, \end{cases} \quad (2.56)$$

for $i = 1, 2$. Then, $v_i(t) \in H_0^2(\Omega)$ for each $0 \leq t \leq T$. Multiplying both sides of (2.52) by $v_1 - v_2$, and integrating over $\Omega \times (0, s)$ yields

$$\begin{aligned} & \int_0^s \int_{\Omega} \left(-(u_1 - u_2)_t (v_1 - v_2)_t - \lambda (u_1 - u_2) (v_1 - v_2)_t + \beta_1 \nabla^2 (u_1 - u_2) \nabla^2 (v_1 - v_2) \right) dx dt \\ & = \int_0^s \int_{\Omega} (\beta_1 - \beta_2) \nabla^2 u_2 \nabla^2 (v_1 - v_2) dx dt. \end{aligned} \quad (2.57)$$

Now, $(v_i)_t = -u$ ($0 < t < T$), and so

$$\begin{aligned} & \frac{1}{2} \int_{\Omega} |(u_1 - u_2)(\cdot, s)|^2 dx + \int_0^s \int_{\Omega} \lambda |u_1 - u_2|^2 dx dt + \frac{1}{2} \int_{\Omega} \beta_1(\cdot, 0) |\nabla^2 (v_1 - v_2)(\cdot, 0)|^2 dx \\ & = \int_0^s \left(\int_{\Omega} (\beta_1 - \beta_2) \nabla^2 u_2 \nabla^2 (v_1 - v_2) dx + \frac{1}{2} \int_{\Omega} |\nabla^2 (v_1 - v_2)|^2 \frac{\partial \beta_1}{\partial t} dx \right) dt. \end{aligned} \quad (2.58)$$

As seen in the proof of Lemma 2.5, there exists positive constants C_3 and C_4 are positive constant depending on B_{σ} , Ω , T and $\|u_0\|_{H^2(\Omega)}$ such that

$$C_3 \leq \beta_i(\cdot, 0) \leq 1, \quad C_3 \leq \beta_i \leq 1, \quad |(\beta_1)_t| \leq C_4, \quad x \in \Omega, \text{ a.e. } t \in (0, T), \quad i = 1, 2, \quad (2.59)$$

which imply from (2.58),

$$\begin{aligned} & \frac{1}{2} \int_{\Omega} |(u_1 - u_2)(\cdot, s)|^2 dx + \int_0^s \int_{\Omega} \lambda |u_1 - u_2|^2 dx dt + \frac{C_3}{2} \int_{\Omega} |\nabla^2 (v_1 - v_2)(\cdot, 0)|^2 dx \\ & \leq \int_0^s \left(\|\beta_1 - \beta_2\|_{L^\infty(\Omega)} \left(\int_{\Omega} |\nabla^2 u_2|^2 dx \right)^{1/2} \left(\int_{\Omega} |\nabla^2 (v_1 - v_2)|^2 dx \right)^{1/2} \right. \\ & \quad \left. + \frac{C_4}{2} \int_{\Omega} |\nabla^2 (v_1 - v_2)|^2 dx \right) dt. \end{aligned} \quad (2.60)$$

By using the Young inequality to (2.60), we obtain

$$\begin{aligned} & \frac{1}{2} \int_{\Omega} |(u_1 - u_2)(\cdot, s)|^2 dx + \int_0^s \int_{\Omega} \lambda |u_1 - u_2|^2 dx dt + \frac{C_3}{2} \int_{\Omega} |\nabla^2 (v_1 - v_2)(\cdot, 0)|^2 dx \\ & \leq C \int_0^s \left(\left(\int_{\Omega} |u_1 - u_2|^2 dx \right)^{1/2} \left(\int_{\Omega} |\nabla^2 (v_1 - v_2)|^2 dx \right)^{1/2} + \int_{\Omega} |\nabla^2 (v_1 - v_2)|^2 dx \right) dt \\ & \leq C \int_0^s \left(\int_{\Omega} |u_1 - u_2|^2 dx + \int_{\Omega} |\nabla^2 (v_1 - v_2)|^2 dx \right) dt. \end{aligned} \quad (2.61)$$

Now, let us write

$$w_i(\cdot, t) = \int_0^t u_i(\cdot, \tau) d\tau, \quad 0 < t < T, \quad (2.62)$$

whereupon (2.61) can be rewritten as

$$\begin{aligned} & \frac{1}{2} \int_{\Omega} |(u_1 - u_2)(\cdot, s)|^2 dx + \int_0^s \int_{\Omega} \lambda |(u_1 - u_2)|^2 dx dt + \frac{C_3}{2} \int_{\Omega} |\nabla^2(w_1 - w_2)(\cdot, s)|^2 dx \\ & \leq C \int_0^s \left(\int_{\Omega} |u_1 - u_2|^2 dx + \int_{\Omega} |\nabla^2(w_1 - w_2)(\cdot, s) - \nabla^2(w_1 - w_2)(\cdot, t)|^2 dx \right) dt. \end{aligned} \quad (2.63)$$

Note that

$$\begin{aligned} & \left\| \nabla^2(w_1 - w_2)(\cdot, s) - \nabla^2(w_1 - w_2)(\cdot, t) \right\|_{L^2(\Omega)}^2 \\ & \leq 2 \left\| \nabla^2(w_1 - w_2)(\cdot, s) \right\|_{L^2(\Omega)}^2 + 2 \left\| \nabla^2(w_1 - w_2)(\cdot, t) \right\|_{L^2(\Omega)}^2. \end{aligned} \quad (2.64)$$

Therefore, (2.63) implies

$$\begin{aligned} & \frac{1}{2} \int_{\Omega} |(u_1 - u_2)(\cdot, s)|^2 dx + \int_0^s \int_{\Omega} \lambda |(u_1 - u_2)|^2 dx dt + \frac{C_3}{2} \int_{\Omega} |\nabla^2(w_1 - w_2)(\cdot, s)|^2 dx \\ & \leq C \int_0^s \left(\int_{\Omega} |u_1 - u_2|^2 dx + 2 \int_{\Omega} |\nabla^2(w_1 - w_2)(\cdot, t)|^2 dx \right) dt \\ & \quad + 2C_s \left\| \nabla^2(w_1 - w_2)(\cdot, s) \right\|_{L^2(\Omega)}^2. \end{aligned} \quad (2.65)$$

Choose T_1 so small such that

$$\frac{C_3}{2} - 2CT_1 \geq \frac{C_3}{4}. \quad (2.66)$$

Then, if $0 < s \leq T_1$, we have

$$\begin{aligned} & \frac{1}{2} \int_{\Omega} |(u_1 - u_2)(\cdot, s)|^2 dx + \int_0^s \int_{\Omega} \lambda |(u_1 - u_2)|^2 dx dt + \int_{\Omega} |\nabla^2(w_1 - w_2)(\cdot, s)|^2 dx \\ & \leq C \int_0^s \left(\int_{\Omega} |u_1 - u_2|^2 dx + 2 \int_{\Omega} |\nabla^2(w_1 - w_2)(\cdot, t)|^2 dx \right) dt. \end{aligned} \quad (2.67)$$

Consequently, the integral form of the Gronwall inequality implies $u_1 - u_2 \equiv 0$ on $(0, T_1]$.

Finally, we apply the same argument on the intervals $(T_1, T_2]$, $(2T_1, 3T_1]$, and so forth and eventually deduce that $u_1 \equiv u_2$ on $(0, T)$. Thus, we obtain the uniqueness of weak solutions. \square

3. Discretised Numerical Scheme

In this section, we construct an explicit discrete scheme to numerically solve differential equation (2.1)–(2.3). Assume a space grid size of h and a time step size of τ , we quantize the space and time coordinates as follows:

$$\begin{aligned} t &= n * \tau, \quad n = 0, 1, 2, \dots, \\ x &= i * h, \quad i = 0, 1, 2, \dots, N, \\ y &= j * h, \quad j = 0, 1, 2, \dots, M, \end{aligned} \quad (3.1)$$

where $M \times N$ is the size of the image. Let $u_{i,j}^n$ be the approximation to the value $u(ih, jh, n\tau)$. We then use a five-step approach to calculate (2.1)–(2.3).

(a) calculating the Laplace of the image intensity functions

$$\begin{aligned} \nabla^2 u_{i,j}^n &= 0.5 \left[\frac{u_{i+1,j}^n + u_{i-1,j}^n + u_{i,j-1}^n + u_{i,j+1}^n - 4u_{i,j}^n}{h^2} \right] \\ &+ 0.25 \left[\frac{u_{i+1,j+1}^n + u_{i-1,j+1}^n + u_{i+1,j-1}^n + u_{i-1,j-1}^n - 4u_{i,j}^n}{h^2} \right], \end{aligned} \quad (3.2)$$

with symmetric boundary conditions

$$\begin{aligned} u_{-1,j}^n &= u_{0,j}^n, u_{N+1,j}^n = u_{N,j}^n, \quad j = 0, 1, 2, \dots, N, \\ u_{i,-1}^n &= u_{i,0}^n, u_{i,M+1}^n = u_{i,M}^n, \quad i = 0, 1, 2, \dots, M, \end{aligned} \quad (3.3)$$

(b) calculating the value of the following function

$$\varphi_{i,j}^n = c_2 \left(\left| \nabla^2 u_{i,j}^n \right| \right) \nabla^2 u_{i,j}^n, \quad (3.4)$$

(c) calculating the Laplace of $\varphi_{i,j}^n$ as

$$\begin{aligned} \nabla^2 \varphi_{i,j}^n &= 0.5 \left[\frac{\varphi_{i+1,j}^n + \varphi_{i-1,j}^n + \varphi_{i,j-1}^n + \varphi_{i,j+1}^n - 4\varphi_{i,j}^n}{h^2} \right] \\ &+ 0.25 \left[\frac{\varphi_{i+1,j+1}^n + \varphi_{i-1,j+1}^n + \varphi_{i+1,j-1}^n + \varphi_{i-1,j-1}^n - 4\varphi_{i,j}^n}{h^2} \right], \end{aligned} \quad (3.5)$$

with symmetry boundary conditions

$$\begin{aligned} \varphi_{-1,j}^n &= \varphi_{0,j}^n, \varphi_{N+1,j}^n = \varphi_{N,j}^n, \quad j = 0, 1, 2, \dots, N, \\ \varphi_{i,-1}^n &= \varphi_{i,0}^n, \varphi_{i,M+1}^n = \varphi_{i,M}^n, \quad i = 0, 1, 2, \dots, M, \end{aligned} \quad (3.6)$$

(d) defining the discrete approximation:

$$\delta u_{i,j}^n = \frac{u_{i,j}^n - u_{i,j}^{n-1}}{\tau}, \quad \delta^2 u_{i,j}^n = \frac{\delta u_{i,j}^n - \delta u_{i,j}^{n-1}}{\tau}, \quad (3.7)$$

with

$$u_{i,j}^0 = u_{i,j}^{-1}, \quad i = 0, 1, 2, \dots, M, \quad j = 0, 1, 2, \dots, N, \quad (3.8)$$

(e) finally, the numerical approximation to the differential equation (2.1) is given as

$$\alpha \delta^2 u_{i,j}^n + \beta \delta u_{i,j}^n = -\nabla^2 \varphi_{i,j}^{n-1}. \quad (3.9)$$

4. Experimental Results

In this section, we present numerical results obtained by applying our proposed fourth-order TDE to image denoising. We test the proposed method on “Barbara” image with size 225×225 (taken from USC-SIPI image database) and “license plate” image with size 240×306 . These two images are shown in Figure 1(a) and Figure 3(a), respectively. The value chosen for the time step size τ is 0.25. To quantify the achieved performance improvements, we adopt improvement in signal to noise ratio (ISNR), which is defined as

$$\text{ISNR} = 10 \cdot \log_{10} \left(\frac{\sum_{i,j} [u(i,j) - u_0(i,j)]^2}{\sum_{i,j} [u(i,j) - u_{\text{new}}(i,j)]^2} \right), \quad (4.1)$$

where $u_0(\cdot)$ is the initial image (noised image) and $u_{\text{new}}(\cdot)$ is the denoised image. The value of ISNR is large, and the restored image is better.

We first study the effects of damping coefficient λ . Figure 1(a) shows the noisy “Barbara” image. Figures 1(c)–1(f) show the restored image using fourth-order TDE ($k = 0.5$, $a = 4$) with $\lambda = 1, 40, 70$ and 100 , respectively. In Figure 2, we plot the ISNR with different damping coefficient λ . We can see that the INSR reaches a maximum at $\lambda = 40$. The INSR value using fourth-order TDE is lower than INSR value using proposed domain-based fourth-order PDE at $\lambda < 9.5$. When $\lambda \rightarrow 100$, the ISNR with fourth-order TDE is almost equal to the ISNR with domain-based fourth-order PDE.

Next, we test the proposed method for image restoration on 50 synthetic degraded images generated using random white Gaussian noise of variance $\sigma = 20$. To verify the effectiveness of our proposed fourth-order TDE method for image restoration, it was evaluated in comparison with PM model [1], TDE model [22], and ITDE model [23]. Figure 3(a) shows the original “License plate” image with size 240×306 . We then added random white Gaussian noise of variance $\sigma = 20$ to generate 50 degraded image. One such degraded image is shown in Figure 3(b). The results yield by PM second-order PDE is shown in Figure 3(c). We observe that “PM second-order PDE” can cause the processed image look block. The results yield by TDE and ITDE are shown in Figures 3(d) and 3(e), respectively. There two methods can leave much more sharp edges than PM second-order PDE but inherits

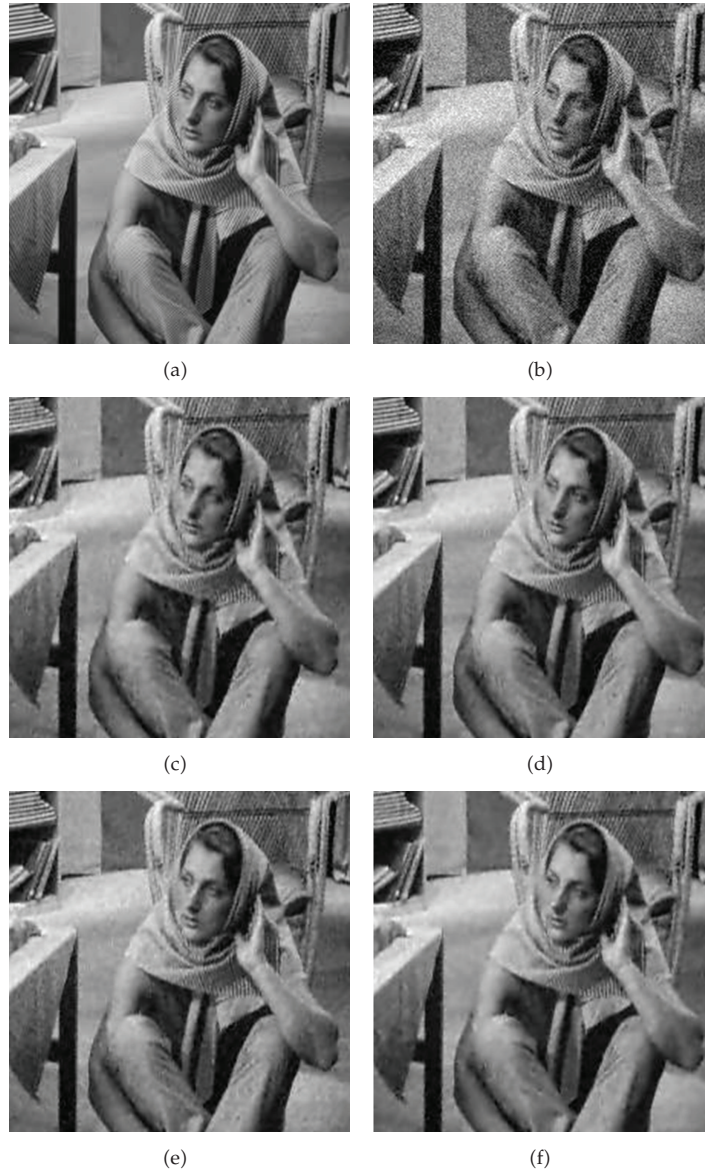


Figure 1: Comparison of different methods on “Barbara” image. (a) Original image. (b) Noised image. (c) Fourth-order TDE with $\lambda = 1$. (d) Fourth-order TDE with $\lambda = 40$. (e) Fourth-order TDE with $\lambda = 70$. (f) Fourth-order TDE with $\lambda = 100$.

the blocky effects from PM second-order PDE to some degree. Figure 3(f) is the restored image using our proposed fourth-order TDE. For the 50 random generated images, the mean of ISNR values for PM, TDE, ITDE, and our proposed fourth-order TDE are 5.7123, 5.8594, 5.9041, and 6.1688, respectively. Table 1 gives 10 of the 50 ISNR values. From Figure 3 and Table 1, we can conclude that our proposed method performs the best quality.

Finally, we designed to further evaluate the good behavior of our proposed fourth-order TDE with white Gaussian noise across 5 noise levels. We added Gaussian white

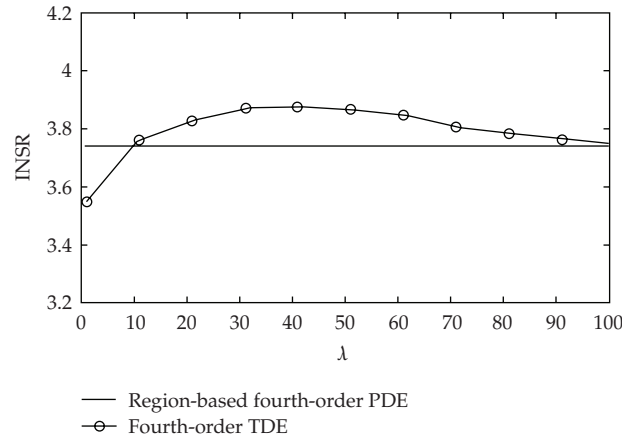


Figure 2: Graph of ISNR versus different damping coefficient λ for "Barbara".

Table 1: ISNR (in dB) values for "license plate" image using random white Gaussian noise of variance $\sigma = 20$.

method	1	2	3	4	5	6	7	8	9	10
PM model	5.7246	5.7309	5.7447	5.7127	5.7502	5.7354	5.7447	5.7049	5.7254	5.5188
TDE model	5.8335	5.8536	5.8443	5.8751	5.8271	5.6747	5.8327	5.8573	5.8767	5.8187
ITDE model	5.9147	5.9152	5.9217	5.9109	5.9198	5.9107	5.9122	5.9098	5.9150	5.9112
Fourth-order TDE	6.1719	6.1382	6.1641	6.1268	6.1626	6.1431	6.1543	6.1797	6.1162	6.1883

Table 2: ISNR (in dB) values for "license plate" image using different methods across five noise levels.

Method	With Gaussian white noise				
	$\sigma = 10$	$\sigma = 15$	$\sigma = 20$	$\sigma = 25$	$\sigma = 30$
PM model	6.9930	6.5647	5.7246	4.9859	4.3677
TDE model	7.1032	6.6143	5.8335	5.1291	4.5038
ITDE model	7.2165	6.8372	5.9147	5.3022	4.6195
Fourth-order TDE	7.3648	6.9296	6.1719	5.5536	4.8564

noise across five different variances σ to the original image. The ISNR values are given in Table 2. Our method obtains higher ISNR than the original method. Furthermore, a ISNR analysis conducted on the standard test image taken from USC-SIPI image database (<http://sipi.usc.edu/database/>) is listed in Table 3. We also note that our method obtains higher mean of ISNR than the original methods.

5. Conclusions

A class of nonlinear fourth-order telegraph-diffusion equation (TDE) for image restoration is presented in this paper. The proposed model first extends the second order TDE for image restoration to fourth-order TDE. Moreover, our proposed model combines nonlinear fourth-order TDE with bilateral filtering, which is not only edge preserving and robust to noise but also avoids the staircase effects. Finally, we study the existence, uniqueness, and stability of the proposed model. A set of numerical experiments is presented to show the good



Figure 3: Comparison of different methods on “License plate” image. (a) Original image. (b) Noisy image. (c) PM smodel with $k = 10$. (d) TDE model with $k = 10, \lambda = 40$. (e) ITDE model with $k = 10, \lambda = 40, \sigma_1 = 0.1$. (f) Proposed fourth-order TDE with $k = 1, a = 4, \lambda = 10$.

Table 3: The mean of ISNR (in dB) values for eight standard test images using random white Gaussian noise of variance 20.

Methods	Noise images					
	Lena	Boats	Camerman	Peppers	House	Elaine
PM model	4.3275	4.1487	4.0326	5.1120	4.2726	5.1737
TDE model	4.4662	4.2745	4.1689	5.2022	4.3996	5.2461
ITDE model	4.5743	4.3948	4.2917	5.2872	4.5127	5.3830
Fourth-order TDE	4.7125	4.5222	4.4134	5.4431	4.6475	5.5705

performance of our proposed model. Numerical results indicate that the proposed model recovers well edges and reduces noise. In [28, 29], the authors point out that the main disadvantage of higher order methods is the complexity of computation. In the future, we will explore a fast and efficient algorithm for our proposed fourth-order TDE method.

Acknowledgments

This work was supported by National Natural Science Foundation of China under Grant no. 60972001 and National Key Technologies R & D Program of China under Grant no. 2009BAG13A06. The authors would like to acknowledge Professor Qilin Liu and Yuxiang Li from Department of Mathematics for many fruitful discussions. The authors also thank the anonymous reviewer for his or her constructive and valuable comments, which helped in improving the presentation of our work.

References

- [1] P. Perona and J. Malik, "Scale-space and edge detection using anisotropic diffusion," *IEEE Transactions on Pattern Analysis and Machine Intelligence*, vol. 12, no. 7, pp. 629–639, 1990.
- [2] F. Catté, P.-L. Lions, J.-M. Morel, and T. Coll, "Image selective smoothing and edge detection by nonlinear diffusion," *SIAM Journal on Numerical Analysis*, vol. 29, no. 1, pp. 182–193, 1992.
- [3] G. W. Wei, "Generalized Perona-Malik equation for image restoration," *IEEE Signal Processing Letters*, vol. 6, no. 7, pp. 165–167, 1999.
- [4] L. I. Rudin, S. Osher, and E. Fatemi, "Nonlinear total variation based noise removal algorithms," *Physica D*, vol. 60, no. 1–4, pp. 259–268, 1992.
- [5] B. B. Kimia, A. Tannenbaum, and S. W. Zucker, "On the evolution of curves via a function of curvature. I. The classical case," *Journal of Mathematical Analysis and Applications*, vol. 163, no. 2, pp. 438–458, 1992.
- [6] Y. L. You, W. Xu, A. Tannenbaum, and M. Kaveh, "Behavioral analysis of anisotropic diffusion in image processing," *IEEE Transactions on Image Processing*, vol. 5, no. 11, pp. 1539–1553, 1996.
- [7] K. Joo and S. Kim, "PDE-based image restoration, I: anti-staircasing and anti-diffusion," Tech. Rep. 2003-07, Department of Mathematics, University of Kentucky, 2003.
- [8] J. Savage and K. Chen, "On multigrids for solving a class of improved total variation based staircasing reduction models," in *Image Processing Based on Partial Differential Equations: Mathematics and Visualization*, Math. Vis., pp. 69–94, Springer, Berlin, Germany, 2007.
- [9] E. Bae, J. Shi, and X.-C. Tai, "Graph cuts for curvature based image denoising," *IEEE Transactions on Image Processing*, vol. 20, no. 5, pp. 1199–1210, 2011.
- [10] Q. Chen, P. Montesinos, Q. S. Sun, and D. Shen Xia, "Ramp preserving Perona-Malik model," *Signal Processing*, vol. 90, no. 6, pp. 1963–1975, 2010.
- [11] Y. Shih, C. Rei, and H. Wang, "A novel PDE based image restoration: convection-diffusion equation for image denoising," *Journal of Computational and Applied Mathematics*, vol. 231, no. 2, pp. 771–779, 2009.
- [12] Y.-L. You and M. Kaveh, "Fourth-order partial differential equations for noise removal," *IEEE Transactions on Image Processing*, vol. 9, no. 10, pp. 1723–1730, 2000.
- [13] M. Lysaker, A. Lundervold, and X. C. Tai, "Noise removal using fourth-order partial differential equation with applications to medical magnetic resonance images in space and time," *IEEE Transactions on Image Processing*, vol. 12, no. 12, pp. 1579–1589, 2003.
- [14] Q. Liu, Z. Yao, and Y. Ke, "Entropy solutions for a fourth-order nonlinear degenerate problem for noise removal," *Nonlinear Analysis: Theory, Methods & Applications*, vol. 67, no. 6, pp. 1908–1918, 2007.
- [15] J. B. Greer and A. L. Bertozzi, " H^1 solutions of a class of fourth order nonlinear equations for image processing," *Discrete and Continuous Dynamical Systems. Series A*, vol. 10, no. 1-2, pp. 349–366, 2004.
- [16] J. B. Greer and A. L. Bertozzi, "Traveling wave solutions of fourth order PDEs for image processing," *SIAM Journal on Mathematical Analysis*, vol. 36, no. 1, pp. 38–68, 2004.

- [17] Q. Liu, Z. Yao, and Y. Ke, "Solutions of fourth-order partial differential equations in a noise removal model," *Electronic Journal of Differential Equations*, no. 120, pp. 1–11, 2007.
- [18] S. Didas, J. Weickert, and B. Burgeth, "Properties of higher order nonlinear diffusion filtering," *Journal of Mathematical Imaging and Vision*, vol. 35, no. 3, pp. 208–226, 2009.
- [19] M. Lysaker and X. C. Tai, "Iterative image restoration combining total variation minimization and a second-order functional," *International Journal of Computer Vision*, vol. 66, no. 1, pp. 5–18, 2006.
- [20] F. Li, C. Shen, J. Fan, and C. Shen, "Image restoration combining a total variational filter and a fourth-order filter," *Journal of Visual Communication and Image Representation*, vol. 18, no. 4, pp. 322–330, 2007.
- [21] D. Yi and S. Lee, "Fourth-order partial differential equations for image enhancement," *Applied Mathematics and Computation*, vol. 175, no. 1, pp. 430–440, 2006.
- [22] V. Ratner and Y. Y. Zeevi, "Image enhancement using elastic manifolds," in *the 14th Edition of the International Conference on Image Analysis and Processing (ICIAP '07)*, pp. 769–774, September 2007.
- [23] Y. Cao, J. Yin, Q. Liu, and M. Li, "A class of nonlinear parabolic-hyperbolic equations applied to image restoration," *Nonlinear Analysis: Real World Applications*, vol. 11, no. 1, pp. 253–261, 2010.
- [24] C. Tomasi and R. Manduchi, "Bilateral filtering for gray and color images," in *Proceedings of IEEE International Conference on Computer Vision*, pp. 839–846, Bombay, India, January 1998.
- [25] M. Zhang and B. K. Gunturk, "Multiresolution bilateral filtering for image denoising," *IEEE Transactions on Image Processing*, vol. 17, no. 12, pp. 2324–2333, 2008.
- [26] L. C. Evans, *Partial Differential Equations*, vol. 19 of *Graduate Studies in Mathematics*, American Mathematical Society, Providence, RI, USA, 1998.
- [27] R. A. Adams, *Sobolev Spaces*, vol. 6 of *Pure and Applied Mathematics*, Academic Press, London, UK, 1975.
- [28] N. Komodakis and N. Paragios, "Beyond pairwise energies: efficient optimization for higher-order mrfs," in *IEEE Computer Society Conference on Computer Vision and Pattern Recognition Workshops (CVPR '09)*, pp. 2985–2992, June 2009.
- [29] X. C. Tai, J. Hahn, and G. J. Chung, "A fast algorithm for Euler's elastic model using augmented Lagrangian method," *SIAM Journal on Imaging Sciences*, vol. 4, pp. 313–344, 2011.



Hindawi

Submit your manuscripts at
<http://www.hindawi.com>

